Journal of Engineering and Applied Sciences 11 (12): 2781-2787, 2016
ISSN: 1816-949X

The Effect of Rotational Speed on Wear Rate of Friction Stir Welding for Joining Aluminium Composite ALSI-SIC

Septian Sigit Setiawan, Rifky Ismail and Sulardjaka
Department of Mechanical Engineering, Faculty of Engineering, Diponegoro University,
Jl. Prof. Sudharto, SH., 50275 Tembalang-Semarang, Semarang, Indonesia

Abstract: The purpose of this investigation is to study the effect of contact between tool and composite on wear rate of the tool shoulder in friction stir welding process. Wear rate was investigated from a weight loss of the tool shoulder after the welding process for each composites. Elevated temperature was measured to reveal the relationship between temperature and wear phenomenon. Visual and microstructure studies are utilized to observe the topography in the each tool surface wear phenomenon. FSW process was done at 1080 RPM rotational speed with translational velocity of 5.652 cm sec^{-1} produces a low wear rate that has good wear resistance. The elevated temperature showed 269.9°C at 5 wt.% SiC, 212°C at 7.5 wt.% SiC and 258.3°C at 10 wt.% SiC, at 1080 RPM rotational speed with the translational speed 5.652 cm sec^{-1} on advancing side. Higher elevated temperature decreases the wear rate. This study explains that butt joint process produced high temperature at advancing side than retreating side in each SiC particle composition. Visual and microstructure study mention that at operating speed of 1080 RPM fewer adhesive layer is found and the measurement for the thickness shows value of 0.2331 mm.

Key words: Friction stir welding, metal matrix composite, wear, shoulder, value

INTRODUCTION

In 1991, Friction Stir Welding (FSW), a new joining techinque was developed by The Welding Institute (TWI) of Cambridge, England (Thomas and Nicholas, 1997). FSW is on kind of solid-state joining technique that has popularity in wide variety of industries including the aerospace, railway, land transportation and marine industries. This method often used on low melting point metal alloys such as aluminium (RajKumar *et al*., 2014; Suri, 2014; Masaki *et al*., 2008; Sato *et al*., 1999; Fujimoto *et al*., 2008), copper, titanium (Zhang *et al*., 2008; Mironov *et al*., 2008) and even iron (Sato *et al*., 2007, 2013; Ohashi *et al*., 2009; Ceschini *et al*., 2007; Kumar and Murugan, 2014; Liu *et al*., 2004) and its alloys.

The FSW process composed three phenomena: heating process, deformation process and forging process. A non consumable rotating tool was used, consisting of a pin and shoulder. The shoulder of the tool is forced against the specimen to take action. The rotating tool causes friction and heats the plates so the mechanical strength decreases. Friction stirs weld has fine microstructure, unlike the fusion weld there is no solidification products and the grains in the weld region are equiaxed and highly refined (Dumpala and Lokanadham, 2014).

Only few researches explained tool wear (Wang *et al*., 2014; Park *et al*., 2009) but that occurs in the FSW process to join the metal matrix composite materials is rarely found (Dumpala and Lokanadham, 2014; Lee *et al*., 2006; Bahrami *et al*., 2014; Prado *et al*., 2001, 2003), especially, today where the FSW process for composites more widely used.

To improve the productivity and efficiency a study is needed to determine the wear rate of the tool shoulder in the FSW process of MMC. Wear of the tool shoulder reduced the quality of FSW joining. Controlling wear is done by determining the efficient parameters and the suitable tool material to join the composite material. This study is investigating the effect of rotational speed on the wear rate of the tool shoulder in the FSW process for AlSi-wt.% SiC composite. This written report also observed effect of the gain in heat (elevated temperature) generated during the procedure.

MATERIALS AND METHODS

Experimental: The FSW process moved the x-axis as the translational speed of the welding parameters. Rotational speed was varied with translational velocity that works effectively on each of them. The parameter is used to determine the effective translational speed of the welding

Corresponding Author: Sulardjaka, Department of Mechanical Engineering, Faculty of Engineering, Diponegoro University, Jl. Prof. Sudharto, SH., 50275 Tembalang-Semarang, Semarang, Indonesia

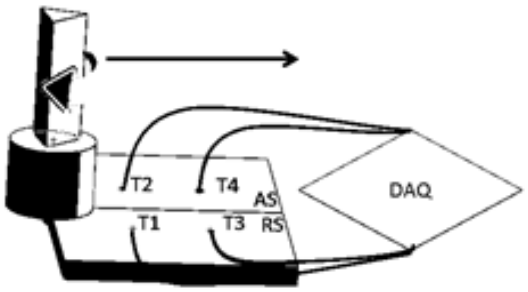

Fig. 1: Schematic of temperature measurement

parameters on every variation each the rotational speed: 808 RPM (7.065 cm sec^{-1}); 1080 RPM (5.642 cm sec^{-1}); and 1540 RPM (4.329 cm sec^{-1}).

AlSi-SiC composites are joined in this study with variations of SiC percentage 5, 7.5 and 10 wt.%. This composites were produced by stir casting method in the previous research. The composite material used is plate-shaped with dimensions (p = 5.4 cm; l = 4 cm and t = 5 mm). Tool material is AISI D2. Tool specifications with a pin-shaped conical with dimension (l_{total}) = 50 mm, ($l_{shoulder}$) = 16 mm, (l_{pin}) = 4 mm and the diameter of specimens ($d_{shoulder}$) = 20 mm, ($d_{pin\ end}$) = 2 mm and ($d_{pin\ base}$) = 4.14 mm.

The method used in this research is the process of joining AlSi-SiC composites with appropriate parameters already mentioned above. After each completed welding process was performed some tests include weight loss, temperature measurement on the surface of the plate and visual observations and microstructure to observe adhesive layer that sticks to the surface of the tool at any rotational speed parameter. After welding process, the weight of each tool was evaluated to calculate the wear rate of tool shoulder.

Welding temperatures were measured on each side of every composites, 2 sensor were placed on the advancing side (T2,T4), another 2 were placed on the retreating side (T1,T3). T1, T2 sensor was placed at a distance 1.8 cm from the initial welds. T3, T4 were placed at a distance 3.6 cm from the initial welds as shown on Fig. 1. Visual (macro) study show which tool was the thickest one. Microstructure study to support the macro study and to show the topography of the surface in every surface of the tool. The microstudy were also used for showing the microstructure of the tool after the welding process then calculating the thickness of adhesive layer.

RESULTS AND DISCUSSION

Weight loss measurement: The data were obtained after the measurement, showed the relationship between wear rate and number of welds, also showed the relationship between wear rate and the rotational speed of the respective percentage of SiC. Figure 2a showed the wear rate on each number of weld. The rotational speed is increased then the wear rate decreased (Fernandez and Murr, 2004; Dwivedi, 2010). The different wear rate on each number of weld because of the different materials, those are AlSi-5 wt.% SiC, AlSi-7.5 wt.% SiC and AlSi-10 wt.% SiC. The different percentage of SiC is shown in Fig. 2b.

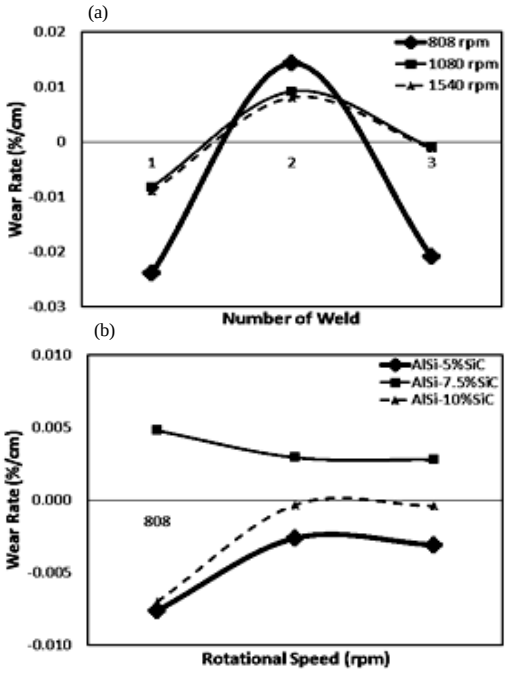

Fig. 2: a) Wear rate diagram and b) wear rate vs. number of weld wear rate vs. rotational speed

In the second weld process the wear rate has positive value. It can be concluded that at second weld, adhesive layer on the surface of tool decreased because it contacted with silicone carbides on every side of this material. The previous study was mentioned that the silicone carbide dispersed evenly. It caused friction in the adhesive layer after first weld and became abrasive wear. Best weld parameters were found at 1080 RPM of rotational speed with 5.652 cm sec^{-1} of translational speed.

Elevated temperature measurement: The temperatures were measured during the welding process of AlSi-SiC composites with the arrangement on the plate T1, T2 at a distance 1.8 cm from the initial weld distance and T3, T4 at a distance of 3.6 cm from the initial weld distance. T1, T3 were placed on the retreating side and T2, T4 were placed on the advancing side.

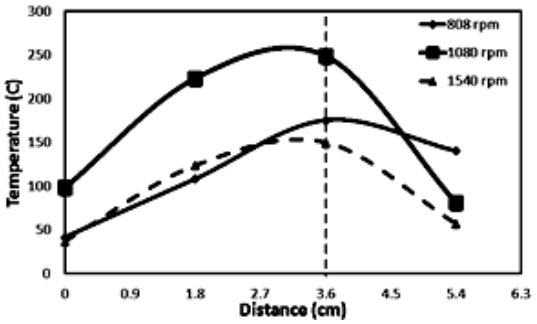

Fig. 3: Relationship diagram between elevated temperature and distance of welding AlSi-5 wt.% SiC

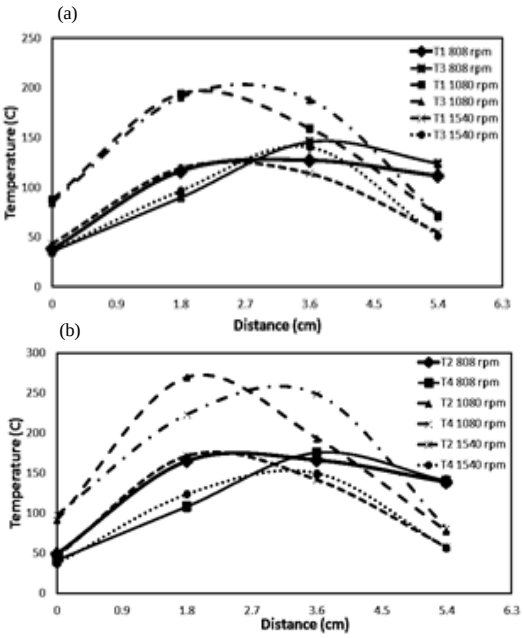

Fig. 4: Elevated temperature vs. distance diagram composite AlSi-5 wt.% SiC on, a) retreating side and b) advancing side

The highest peak temperature measured on each composite was at 1080 RPM of rotational speed with 5.652 cm sec^{-1} translational speed. Higher temperatures decrease the yield strength of the material surface and improve the continuity and thickness of the protective oxidation layer on the surface, the friction occurred and reduced the direct contact between the metal (Dwivedi, 2010). Figure 3-8, the temperature showed at 0 cm weld distance, temperatures were in the range of 30-50°C.

At 1.8 cm from the initial weld position or tool position is in the center between the sensors T1 and T2. The high temperature was on T1(retreating side) and T2 (advancing side), than T3 and T4 were lower. T1 and T2

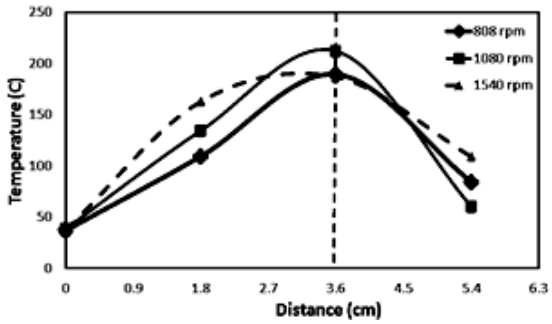

Fig. 5: Relationship diagram between elevated temperature and distance of welding AlSi-7,5 wt.% SiC

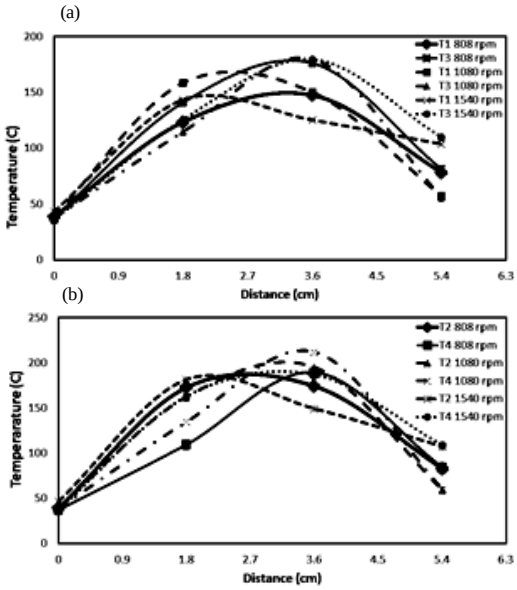

Fig. 6: Elevated temperature vs distance diagram composite AlSi-7,5 wt.% SiC on, a) retreating side and b) advancing side

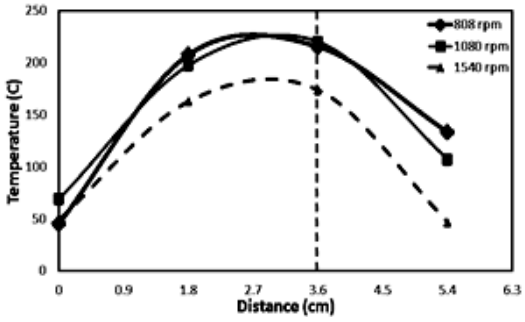

Fig. 7: Relationship diagram between elevated temperature and distance of welding AlSi-10 wt.% SiC

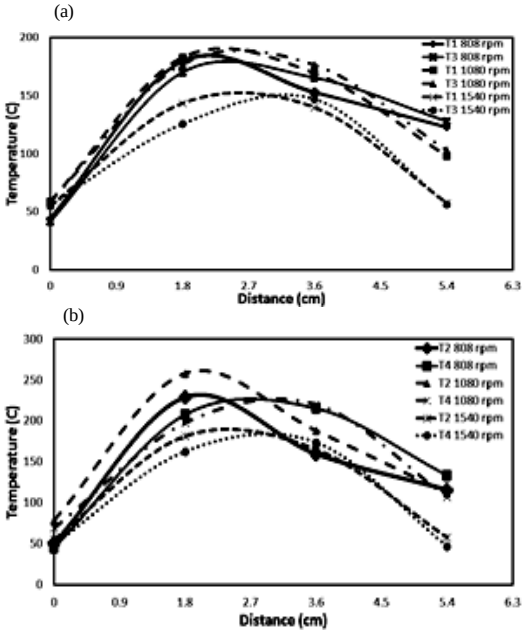

Fig. 8: Elevated temperature vs. distance diagram composite AlSi-10 wt.% SiC on, a) retreating side and b) advancing side

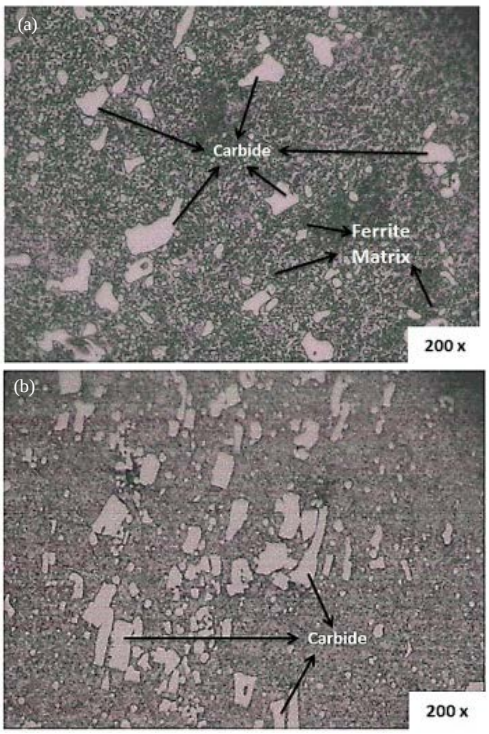

Fig. 9: Micostructure of AISI D2 tool steel, a) before hardening and b) after hardening

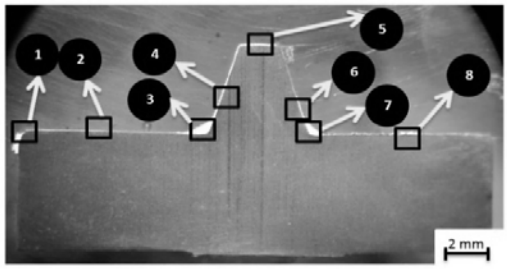

Fig. 10: Topography of surface at 808 RPM rotational speed

The temperature at 1080 RPM of rotational speed has the highest temperature at advancing side for butt joint welding (Maeda *et al*., 2005).

Microstructure and topography study: Visual and microstructure test was conducted to determine the wear phenomenon as a result of adhesive layer on the tool surface. Figure 9 shows the microstructure of the tool steel (a) before hardening and (b) after hardening. Carbides have a larger size after hardening treatment. Tool Material that didn't harden the carbides were formed along the ferrite matrix (Yasavol *et al*., 2014) but after hardening visible light colored was a martensite structure. It made the improvement of hardness, when the hardness increase, the wear phenomenon decreases.

Figure 10 and 11 show the adhesive layer that sticks to the surface of the tool at 808 RPM rotational speed. Existing adhesive layer evenly spread over the entire surface of the tool such as in the shoulder, the angle between the pin and the shoulder and also at pin head.

Adhesive layer as shown in Fig. 12 and 13 attached to the tool with 1080 RPM rotational speed look thin on the surface of the tool. The wear rate on this tool was the thinnest compared with the other. Figure 14 and 15 showed the adhesive layers at some point which are thick on three areas: right and left angle between tool and pin and also at the pin head, there is a hollow at the adhesive layer on the left side of angle so the adhesive layers can not define by its look.

The thickness of adhesive layer on each cutting tool was shown in Fig. 16, there was less adhesive layer at 1080 RPM rotational speed with the value of 0.2231 mm.decrease after passing half way as well as T3 and T4 increase, the tool was at distance 3.6 cm or tool position was on between T3 and T4, showed that T3 (retreating side) and T4 (advancing side) were higher than T1 and T2.

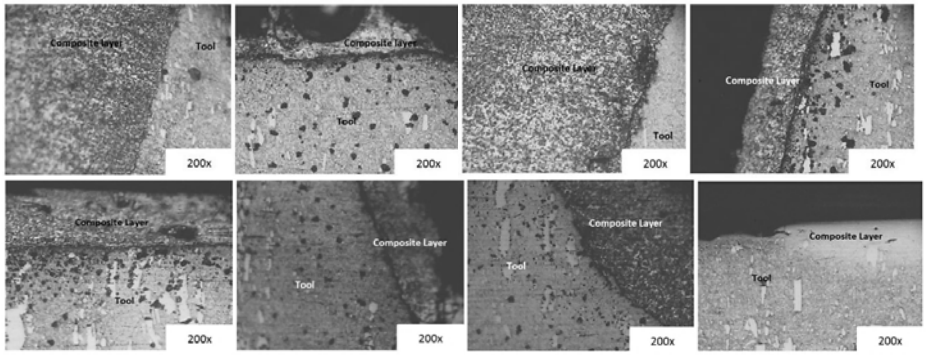

Fig. 11: Microstructure each point at 808 RPM rotational speed

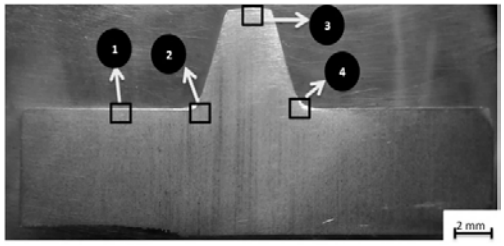

Fig. 12: Topography of surface at 1080 RPM rotational speed

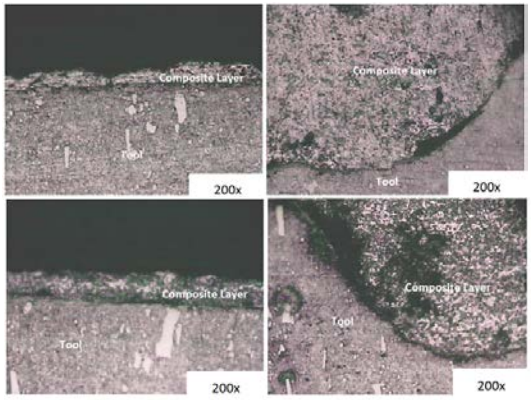

Fig. 13: Microstructure each point at 1080 RPM rotational speed

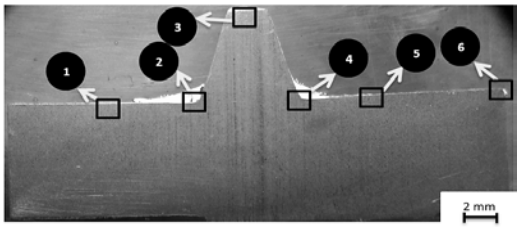

Fig. 14: Topography of surface at 1540 RPM rotational speed

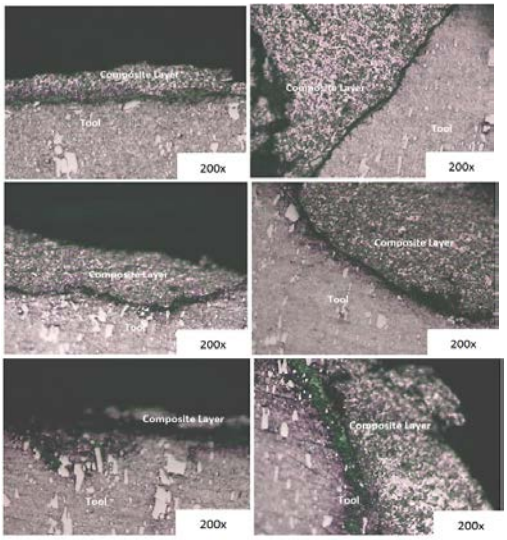

Fig. 15: Microstructure each point at 1540 RPM rotational speed

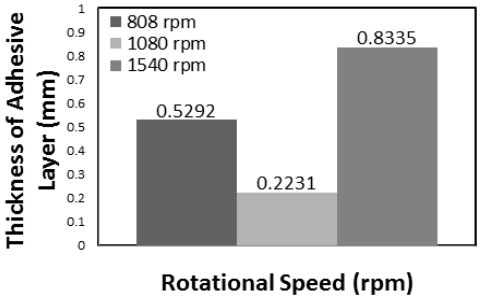

Fig. 16: The thickness of adhesive layer each tool

CONCLUSION

These study can be concluded that the smallest wear rate was in the tool at 1080 RPM of rotational speed

with 7.065 cm sec^{-1} of translational speed. Adhesive wear appeared In the first weld for the composition of 5 wt.% SiC showed the highest value of wear rate, then the second weld for the composition of 7.5 wt.% SiC wear rate decreases. The third weld for composition of 10 wt.% SiC wear rate rises back. At 1080 RPM rotational speed for 7,5 w.t% SiC composition has good mechanical properties. Then the tool weight decreased and adhesive layer reduced. The temperature measurement also showed higher at advancing side. The microstructure and topography image showed that 1080 RPM of rotational speed has less adhesive layer on every surface and the thickness was calculated, it showed less thickness.

ACKNOWLEDGEMENTS

The rsearchers would like to express their gratefulness to the Rector of Diponegoro University who funded this research. With number of research grants: 314-26/UN7.5.1/PG/2015.

REFERENCES

Bahrami, M., K. Dehghani and M.K.B. Givi, 2014. A novel approach to develop aluminum matrix nano-composite employing friction stir welding technique. Mater. Des., 53: 217-225.

Ceschini, L., I. Boromei, G. Minak, A. Morri and F. Tarterini, 2007. Effect of friction stir welding on microstructure, tensile and fatigue properties of the AA7005/10vol.% Al 2 O 3p composite. Compos. Sci. Technol., 67: 605-615.

Dumpala, L. and D. Lokanadham, 2014. Low cost friction stir welding of aluminium nanocomposite-A review. Procedia Mater. Sci., 6: 1761-1769.

Dwivedi, D.K., 2010. Adhesive wear behaviour of cast aluminium-silicon alloys: Overview. Mater. Des., 31: 2517-2531.

Fernandez, G.J. and L.E. Murr, 2004. Characterization of tool wear and weld optimization in the friction-stir welding of cast aluminum 359+ 20% SiC metal-matrix composite. Mater. Charact., 52: 65-75.

Fujimoto, M., S. Koga, N. Abe, Y.S. Sato and H. Kokawa, 2008. Microstructural analysis of stir zone of Al alloy produced by friction stir spot welding. Sci. Technol. Weld. Joining, 13: 663-670.

Kumar, B.A. and N. Murugan, 2014. Optimization of friction stir welding process parameters to maximize tensile strength of stir cast AA6061-T6/AlN p composite. Mater. Des., 57: 383-393.

Lee, W.B., C.Y. Lee, M.K. Kim, J.I. Yoon and Y.J. Kim *et al*., 2006. Microstructures and wear property of friction stir welded AZ91 Mg/SiC particle reinforced composite. Compos. Sci. Technol., 66: 1513-1520.

Liu, H.J., H. Fujii and K. Nogi, 2004. Microstructure and mechanical properties of friction stir welded joints of AC4A cast aluminium alloy. Mater. Sci. Technol., 20: 399-402.

Maeda, M., H. Liu, H. Fujii and T. Shibayanagi, 2005. Temperature field in the vicinity of FSW-tool during friction stir welding of aluminium alloys. Weld. World, 49: 69-75.

Masaki, K., Y.S. Sato, M. Maeda and H. Kokawa, 2008. Experimental simulation of recrystallized microstructure in friction stir welded Al alloy using a plane-strain compression test. Scripta Materialia, 58: 355-360.

Mironov, S., Y. Zhang, Y.S. Sato and H. Kokawa, 2008. Crystallography of transformed β microstructure in friction stir welded Ti-6Al-4V alloy. Scr. Mater., 59: 511-514.

Ohashi, R., M. Fujimoto, S. Mironov, Y.S. Sato and H. Kokawa, 2009. Effect of contamination on microstructure in friction stir spot welded DP590 steel. Sci. Technol. Weld. Joining, 14: 221-227.

Park, S.H.C., Y.S. Sato, H. Kokawa, K. Okamoto and S. Hirano *et al*., 2009. Boride formation induced by pcBN tool wear in friction-stir-welded stainless steels. Metall. Mater. Trans. A, 40: 625-636.

Prado, R.A., L.E. Murr, D.J. Shindo and K.F. Soto, 2001. Tool wear in the friction-stir welding of aluminum alloy 6061+ 20% Al 2 O 3: A preliminary study. Scr. Mater., 45: 75-80.

Prado, R.A., L.E. Murr, K.F. Soto and J.C. McClure, 2003. Self-optimization in tool wear for friction-stir welding of Al 6061+ 20% Al 2 O 3 MMC. Mater. Sci. Eng. A, 349: 156-165.

RajKumar, V., M. VenkateshKannan, P. Sadeesh, N. Arivazhagan and K.D. Ramkumar, 2014. Studies on effect of tool design and welding parameters on the friction stir welding of dissimilar aluminium alloys AA 5052-AA 6061. Procedia Eng., 75: 93-97.

Sato, Y.S., H. Kokawa, M. Enomoto and S. Jogan, 1999. Microstructural evolution of 6063 aluminum during friction-stir welding. Metall. Mater. Trans. A, 30: 2429-2437.

Sato, Y.S., H. Yamanoi, H. Kokawa and T. Furuhara, 2007. Microstructural evolution of ultrahigh carbon steel during friction stir welding. Scr. Mater., 57: 557-560.

Sato, Y.S., N. Harayama, H. Kokawa, H. Inoue and Y. Tadokoro *et al*., 2013. Evaluation of microstructure and properties in friction stir welded superaustenitic stainless steel. Sci. Technol. Weld. Joining, 14: 202-209.

Suri, A., 2014. An improved FSW tool for joining commercial aluminum plates. Procedia Mater. Sci., 6: 1857-1864.

Thomas, W.M. and E.D. Nicholas, 1997. Friction stir welding for the transportation industries. Mater Des., 18: 269-273.

Wang, J., J. Su, R.S. Mishra, R. Xu and J.A. Baumann, 2014. Tool wear mechanisms in friction stir welding of Ti-6Al-4V alloy. Wear, 321: 25-32.

Yasavol, N., A.A. Zadeh, M.T. Vieira and H.R. Jafarian, 2014. Microstructure evolution and texture development in a friction stir-processed AISI D2 tool steel. Appl. Surf. Sci., 293: 151-159.

Zhang, Y., Y.S. Sato, H. Kokawa, S.H.C. Park and S. Hirano, 2008. Stir zone microstructure of commercial purity titanium friction stir welded using pcBN tool. Mater. Sci. Eng. A, 488: 25-30.